The gated gait of the processive molecular motor, myosin V

Claudia Veigel*‡, Fei Wang†, Marc L. Bartoo*, James R. Sellers†§ and Justin E. Molloy*

**Department of Biology, University of York, PO Box 373, York YO10 5YW, UK*
†Laboratory of Molecular Cardiology, National Heart, Lung and Blood Institute, NIH, Bethesda, MD 20892USA
‡e-mail: cv1@york.ac.uk
§e-mail: jsellers@helix.nih.gov

Published online: 10 December 2001, DOI: 10.1038/ncb732

Class V myosins are actin-based molecular motors involved in vesicular and organellar transport. Single myosin V molecules move processively along F-actin, taking several 36-nm steps for each diffusional encounter. Here we have measured the mechanical interactions between mouse brain myosin V and rabbit skeletal F-actin. The working stroke produced by a myosin V head is ~25 nm, consisting of two separate mechanical phases (20 + 5 nm). We show that there are preferred myosin binding positions (target zones) every 36 nm along the actin filament, and propose that the 36-nm steps of the double-headed motor are a combination of the working stroke (25 nm) of the bound head and a biased, thermally driven diffusive movement (11 nm) of the free head onto the next target zone. The second phase of the working stroke (5 nm) acts as a gate — like an escapement in a clock, coordinating the ATPase cycles of the two myosin V heads. This mechanism increases processivity and enables a single myosin V molecule to travel distances of several hundred nanometres along the actin filament.

Class V myosins are two-headed, actin-based motors that use the free energy derived from ATP hydrolysis to produce a wide variety of directed cellular movements including the transport of melanosomes, mRNA, smooth endoplasmic reticulum and neuronal vesicles[1–4]. Previous studies[5–9] have shown that myosin V is a processive motor that moves along a single actin filament by taking several successive 36-nm steps before diffusing from the filament track. However, the detailed mechanism that underlies such processive movement is still not fully understood. Here we address the issue of how the individual mechanical steps are made (that is, the gait of the motor) and provide evidence for a mechanical gating mechanism that reduces the stochastic asynchrony between the chemical cycles of the two heads and enhances the molecular processivity[10].

Mouse brain myosin V consists of two heavy chains, each with an amino-terminal head region composed of a motor domain, a regulatory domain that binds six light chains and a carboxy-terminal tail region that contains coiled-coil-forming motifs (dimerization domain) and a cargo-binding domain[2]. The current view is that during its ATPase cycle, the myosin motor domain attaches to actin, generates force and then detaches. This enables the molecule to advance along actin towards its next actin-binding site. Because myosin V has two heads they might operate in a hand-over-hand fashion to walk or 'process' along actin. This would be a probabilistic process and the degree of processivity, or average 'run length', would depend on the biochemical processes occurring on both heads. When a human being walks, the movement is fairly smooth; this is because inertial forces are large compared with friction. However, the situation is reversed for single motor molecules; momentum is negligible and friction forces dominate. This means that motor proteins should produce a rather jerky motion that consists of discrete steps or dwell points.

We expect a motor molecule to dwell in certain biochemical or mechanical states and make rapid transitions between these states. We know from solution biochemical studies that the acto-myosin ATP hydrolysis pathway consists of many, probably about seven, states. However, let us here consider a simple model in which the biochemical cycle is reduced to two states, one that is attached to actin and the other detached (Fig. 1). The apparent attachment (f) and detachment (g) rate constants then determine the instantaneous probability of a myosin head being attached to actin ($f/(f+g)$). Alternatively, one can consider this as the average proportion of time that a head spends bound during an average catalytic cycle period. This has become known as the duty-cycle ratio, r. If both myosin V heads can bind simultaneously to actin and their biochemical cycles are independent and stochastic, the average number of steps taken per diffusional encounter (which we define here as its processivity number, P_n), will be $P_n = 1 + [\ln 2/-\ln(2r - r^2)]$. This is equal to the average run length divided by the step size. Here we have assumed that a processive run of interactions terminates when, by chance, both heads detach from actin simultaneously (with a probability of $2r - r^2$) (see Fig. 1). By this analysis, low-duty-ratio motors, for example skeletal muscle myosin II, have a P_n of close to one.

Structural studies[8] have shown that the two heads of intact myosin V are long enough for both heads to be able to bind simultaneously to F-actin with spacing between the leading and trailing heads that is commensurate with the actin filament's helical pseudo-repeat distance of 36 nm. This means that both heads can bind with little or no azimuthal distortion (that is, little twist with respect to the actin filament axis). However, there might be other modes of internal strain in the molecule, for example longitudinal bending strain or torsion at the junction between the heads.

Solution biochemical studies of single-headed, recombinant, myosin V have shown that the ATPase cycle has a high duty ratio ($r \geq 0.7$) (ref. 9). The observed rate constant for ADP release is similar to the catalytic site activity (~10 s^{-1}) and is probably rate-limiting for both the ATPase activity and the stepping rate. From our simple model, a duty ratio of 0.7 would predict a P_n of 8.3 steps.

Single-molecule mechanical studies using optical tweezers have allowed both the step size and average run length of the processive motion to be measured directly. The step size, or distance moved between dwells, is reported[5,6] as 36 nm; we find the same value in the present study. In these experiments it has been difficult to measure the processivity number directly for two different reasons. First, in the earliest study[5], processivity was limited because the increasing

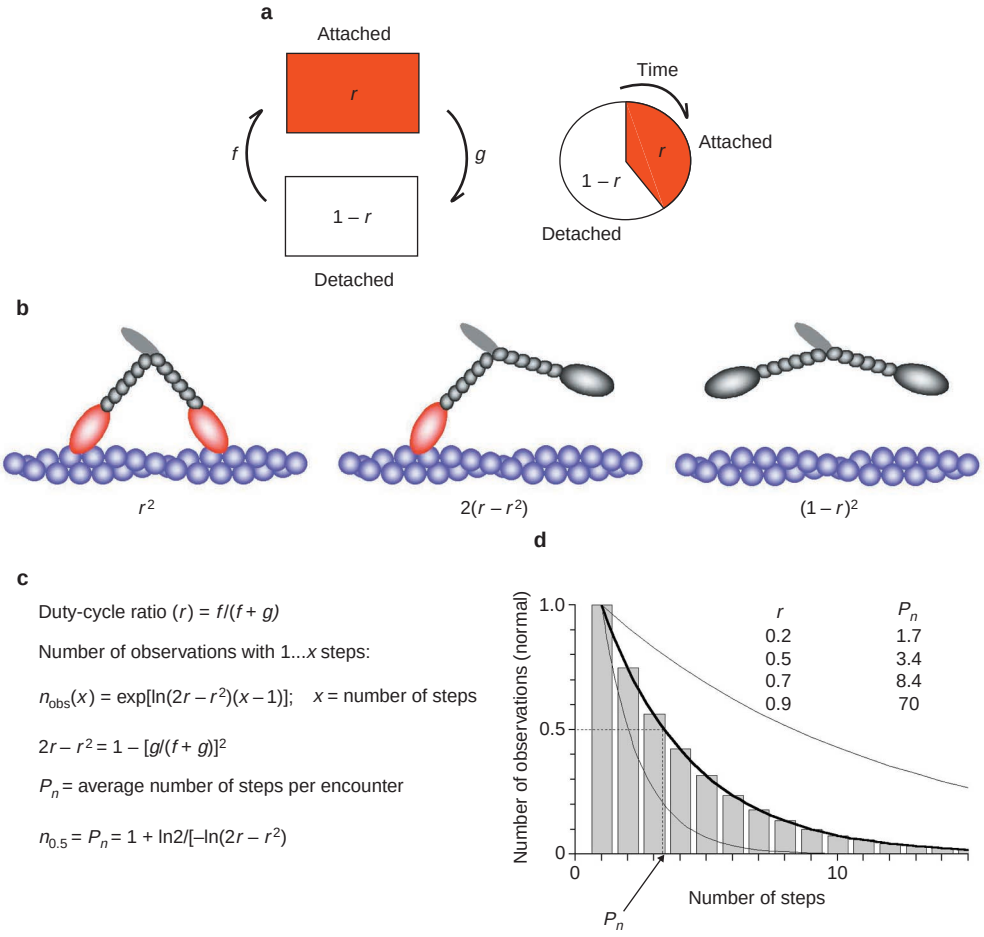

Figure 1 **Duty-cycle ratio of myosin V. a**, How a single myosin head might adopt two states (detached and attached). The rate constants governing transitions between these states are here termed *f* and *g* (ref. 22). The average proportion of time spent in the attached state (known as the duty-cycle ratio, *r*) compared with the total cycle time is shown on the right. **b**, The possible bound configurations for a two-headed myosin species: both heads attached, one head attached and one detached, and both heads detached; immediately below this, the average proportion of time spent in each configuration is shown as a function of *r*. **c**, The dependence of *r* on the rate constants *f* and *g*. **d**, How the expected number of steps taken (degree of processivity) depends on *r*. The processivity number, defined as the average number of steps taken per diffusional encounter, is derived in terms of this simple model (bottom line in **c**). The inset in d shows how the processivity depends on *r* for four arbitrary values of *r*. One important feature of this type of analysis is that all two-headed motors are processive, and the concept of processivity is framed correctly as a continuum.

force applied by the fixed optical tweezer caused myosin V to stall. The stall force was ~3 pN and was reached after only four or five steps. Second, in the more recent study[6] a force-feedback arrangement was used in which a constant small force was applied and runs of up to 10 steps were recorded. However, run length was limited by the range and linearity of the position sensor.

The published mechanical studies have also addressed the issue of how the mechanical and biochemical cycles of myosin V are coupled. They have shown that at low loads and physiological concentration of ATP, velocity is limited by the rate of ADP release from the trailing head[6] and this is made slower by increasing load. In contrast, at low ATP concentration the velocity is limited by the rate of ATP binding and this is relatively insensitive to external load[5].

Single-molecule fluorescence imaging[7] has enabled the run length of single, fluorescently labelled, myosin V molecules to be viewed directly. Individual run lengths were distributed exponentially (like the model graph of Fig. 1) with an average distance of 2.4 μm. So if we combine the results of the single-molecule optical and mechanical studies we find that the processivity number at low load would be 2400/36 = 66 steps.

We expect each processive step to be produced by a single biochemical cycle, in other words the breakdown of one ATP molecule[6]. However, the dwell period at each step could contain several biochemical states and the movement between dwell points (the step itself) might be driven by different biophysical processes. Here we propose that the myosin V mechanical step is produced by a combination of two different processes: a two-phase 'working-stroke' that is produced by a single myosin head while it is attached to actin, and a 'diffusive search' that is produced by the second myosin head while it is detached from actin.

Results

The working stroke of single-headed, recombinant myosin V (MVS1) is produced in two phases. We used a transducer based on optical tweezers[11] to compare the mechanical properties of two forms of mouse-brain myosin V: (1) single-headed recombinant protein (termed MVS1), produced by baculovirus expression[12] and composed solely of the motor domain and neck region with all six-light-chain binding motifs, and (2) tissue-purified[13] intact

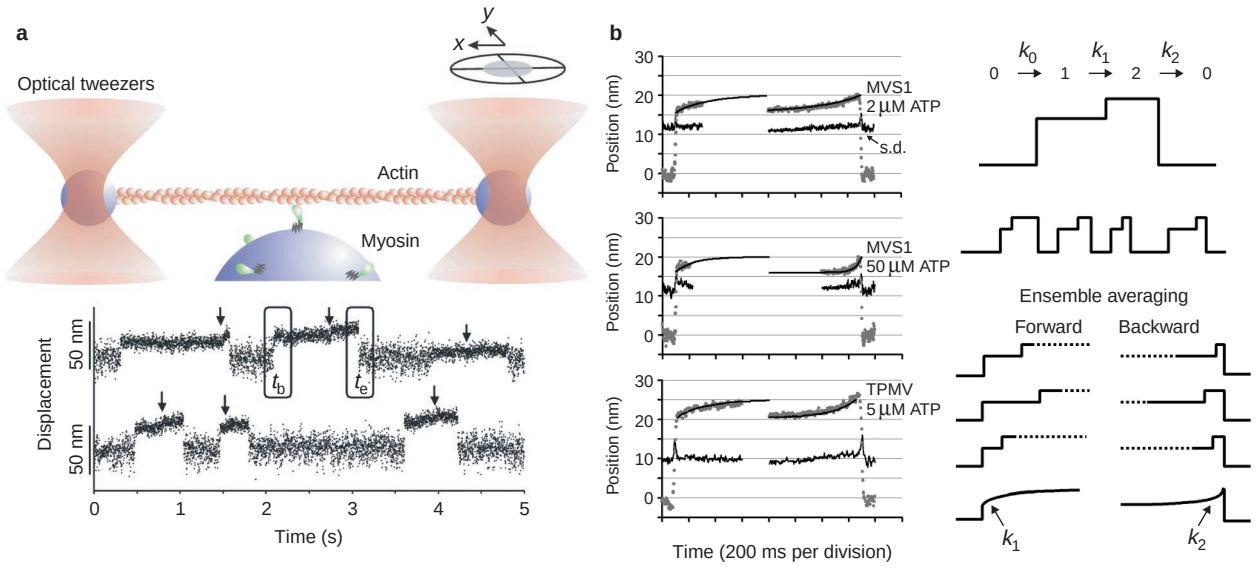

Figure 2 **Single-molecule mechanical interactions measured for MVS1. a**,The record shows bead movement in parallel with the actin filament axis at low trap stiffness (see Methods). Intervals of reduced Brownian noise indicate attachment events of a single MVS1 (ref. 15). During the attachment events a small step occurred with a time delay of ~140 ms after binding (arrows). **b**, Examples of ensemble-averaged attachment events measured with MVS1 at two different ATP concentrations and TPMV (grey data points). Data points were synchronized to the beginning (t_b) and end (t_e) of each attachment event (Fig. 1a) by thresholding the variance of the raw data. The kinetics of the first and second phases of the working stroke were separated in the following way: the kinetics of the first phase (k_1) was obtained by synchronizing n displacement events with respect to the beginning (t_b) of each event; however, before ensemble averaging, all events with lifetime t_n were made to be of the same duration t by extending short events by the time $t - t_n$, keeping the level reached at the end of the event during the extra time $t - t_n$ (bottom right, dotted lines). The kinetics of the second phase (k_2) was obtained by aligning the displacement events with respect to the end (t_e) of each event and again all events were made to be of the same duration t by extending the duration of short events at the beginning of the event. The time course of the ensemble average was fitted by single exponentials. Rate constants determined for MVS1 with 2, 10 and 50 μM ATP, respectively, were as follows: k_1 = 4.5, 5 and 7 s^{-1}; k_2 = 3, 8 and 30 s^{-1}; n = 152, 152 and 136. Rate constants for single-step interactions measured with TPMV were k_1 = 6 s^{-1} and k_2 = 5 s^{-1}, n = 152, for 5 μM ATP. The standard deviation (s.d.) of the ensemble data at each time window is plotted as a black line. The s.d. measured during the event window is the same as that of the data recorded before and after the event. This means that the events do not in themselves add extra variation to the data and the individual event amplitudes must vary by less than 5 nm.

dimeric myosin V (termed TPMV). Both proteins were active in motility assays *in vitro* and moved actin at similar velocities of ~0.3 μm s^{-1}. In our experiments, a single actin filament was suspended between two plastic microspheres held in two optical tweezers (Fig. 2a). The filament was positioned over a third, surface-attached, bead on which myosin V was deposited at a sufficiently low density for single acto-myosin V molecular interactions to occur. Mechanical interactions were measured by monitoring the positions of the microspheres holding the actin filament by using two photodetectors[14] (Fig. 2). MVS1 produced single, isolated interactions with the actin filament, which were identified by the change in Brownian noise[15] of the signal, corresponding to sudden changes in system stiffness as myosin bound to actin. Individual displacements were biased in one direction, determined by the orientation of the actin filament. Close inspection of individual events showed that displacements were produced in two distinct phases. An initial displacement of 16 nm was produced within 10 ms of acto-MVS1 binding; this was followed by a further displacement of 5 nm, which occurred after an average delay of ~140 ms (Fig. 2b). The amplitude and kinetics of the first and second phases were determined by an averaging method[16] (Fig. 2b): individual events were synchronized to their start and end as defined by changes in signal variance. Both the average event amplitude and the transition kinetics between the two mechanical states could then be derived by exponential fitting to the averaged data. The duration of the initial displacement (phase 1) was independent of ATP concentration (with a transition rate constant, k_1, of 5 s^{-1}), whereas the duration of the second displacement (phase 2) became briefer at higher ATP concentration (with a transition rate constant, k_2, of ~1 $\mu M^{-1}s^{-1}$; Fig. 2b). The kinetic parameters are in good agreement with rate constants determined for ADP release and ATP binding measured in solution for MVS1 (refs 9, 13). From these experiments we conclude that a single myosin V head produces a working stroke of 21 nm and that this occurs in two distinct phases.

The working stroke produced by a single myosin V head is significantly shorter than the step size produced by dimeric myosin V. Mechanical experiments with TPMV showed a more complicated behaviour than MVS1. We observed a mixture of isolated single interactions and 'staircase' interactions involving multiple successive steps (Fig. 3a). This behaviour is as expected for a stochastic, processive enzyme that stalls at high load. Our data for TPMV are consistent with a P_n of ~15–20. This value is calculated from the distribution of the number of steps taken in staircases at low load (<2 pN). The frequency of single interactions and short runs with two and three steps indicate that the processivity of myosin V is lower than that of highly processive enzymes such as kinesin or DNA polymerases, which produce hundreds of steps per diffusional encounter. We exploited the relatively low processivity of this enzyme (that is, compared with conventional kinesin) to obtain an estimate of the working stroke amplitude by analysing the small number of single isolated interactions. We assume that interactions giving rise to a single displacement level occur when the second TPMV head fails to bind before the first head has detached; such events therefore enable the working stroke to be determined.

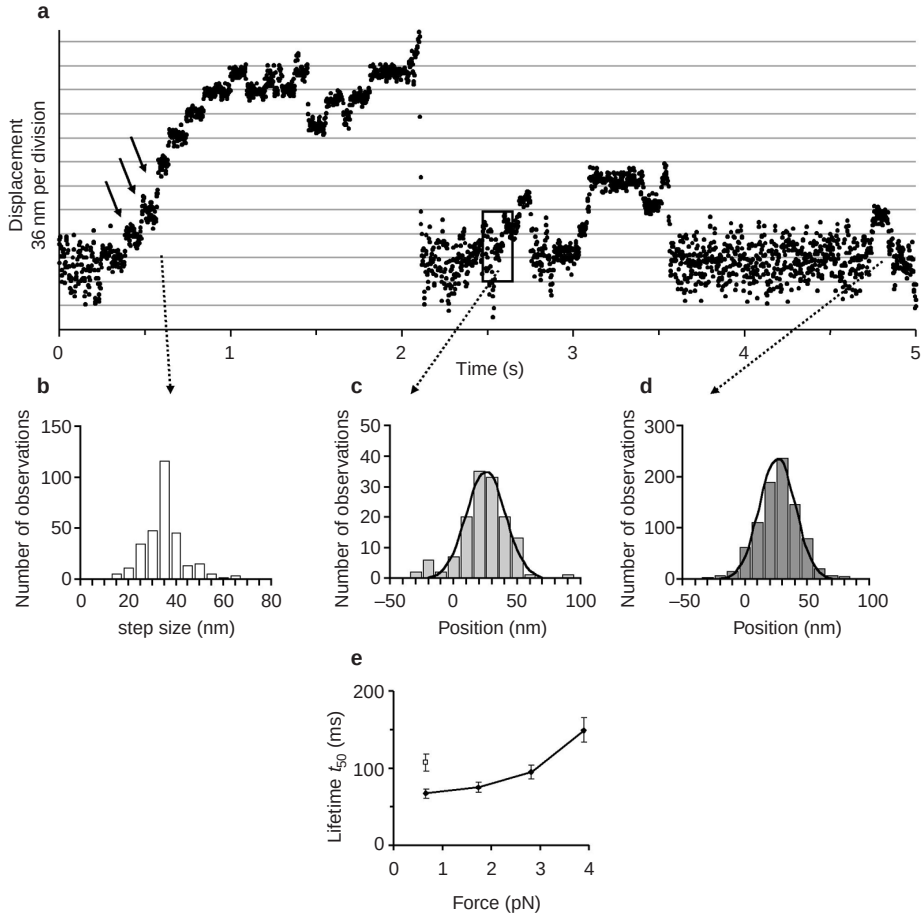

Figure 3 **Single-molecule mechanical interactions measured for TPMV.** **a**, Attachment events with one to nine successive steps ('staircases') were observed (100 μM ATP). **b**, Mean step size of the second to fourth steps in the staircases; mean ± s.e.m. 34.5 ± 0.6 nm, $n = 302$, 100 μM ATP. **c**, Amplitude of the first step in the staircases; mean ± s.e.m. 26.2 ± 2.3 nm, $n = 142$, 100 μM ATP. **d**, Amplitude of single step displacements; mean ± s.e.m. 25.7 ± 0.6 nm, $n = 885$, 5 μM ATP. **e**, Force-dependent lifetime of steps. Filled diamonds show dwell times during staircases; $n = 125$, 127, 107 and 86 for external forces of 0.5, 1.2, 1.9 and 2.7 pN, respectively. The open square shows the dwell time of single interactions of TPMV with actin $n = 885$, average force of 0.77 pN.

We found that the amplitude of such single isolated events and also the first step in a 'staircase' produced by TPMV (Fig. 3c, d) were similar to the isolated interactions produced by MVS1. We conclude that the working stroke of both MVS1 and TPMV is 21–25 nm, whereas the average step size produced by the processive interaction of TPMV is 34–36 nm (Fig. 3b)[3]. We believe that the slightly smaller working stroke measured for MVS1 (21 nm) than the stroke size measured for TPMV (25 nm) is most probably based on slight differences in binding of the two different molecules to the nitrocellulose surface.

Actin scanning experiment. To explore this result further, we used MVS1 to see whether there were preferred or target binding positions along the actin filament, as suggested originally for insect flight muscle[17] and indicated in an earlier study on rabbit skeletal muscle myosin II (ref. 11). We moved the actin filament back and forth, past a single MVS1 molecule, by applying a sinusoidal motion to one of the optical tweezers. This enabled us to probe the binding probability of myosin V along a segment of the actin filament that spanned several of its helical repeats. We then measured the pairwise difference in binding position between adjacent actomyosin binding interactions to see whether binding occurred at discretely spaced sites along actin. We found that adjacent interactions showed 'beating' at multiples of 36 nm (Fig. 4).

Stiffness measurements indicate the number of attached heads during processive interactions. Finally, we measured changes in stiffness and position as TPMV walked along the actin filament (Fig. 5A). To do this we applied a rapid sinusoidal oscillation to one of the beads holding the actin filament and monitored pickup of this signal at the other bead. We found a brief decrease in stiffness from ~0.35 to ~0.18 pN nm^{-1} immediately preceding many of the transitions between step levels. At low load (<1 pN), the dwell time at reduced stiffness was ~18 ms, although at high load (>2 pN) intervals of reduced stiffness increased to hundreds of milliseconds. We interpret intervals of high stiffness to be those in which both heads are bound and the brief intervals of low stiffness to be those in which only one head is bound. In separate experiments with MVS1 we found the stiffness with one myosin head bound to be 0.2 ± 0.01 pN nm^{-1} (mean ± s.e.m.; $n = 47$; 5 μM ATP; data not shown).

Discussion

One way of explaining the disparity between the step size (34–36 nm) and the work-stroke size (21–25 nm) is if the step is produced by a combination of (1) a working stroke produced when myosin is bound to actin and (2) forward-biased diffusion of the unbound head onto the next 'preferred' or 'target' actin monomer. The diffusive component would show directional bias only in measurements

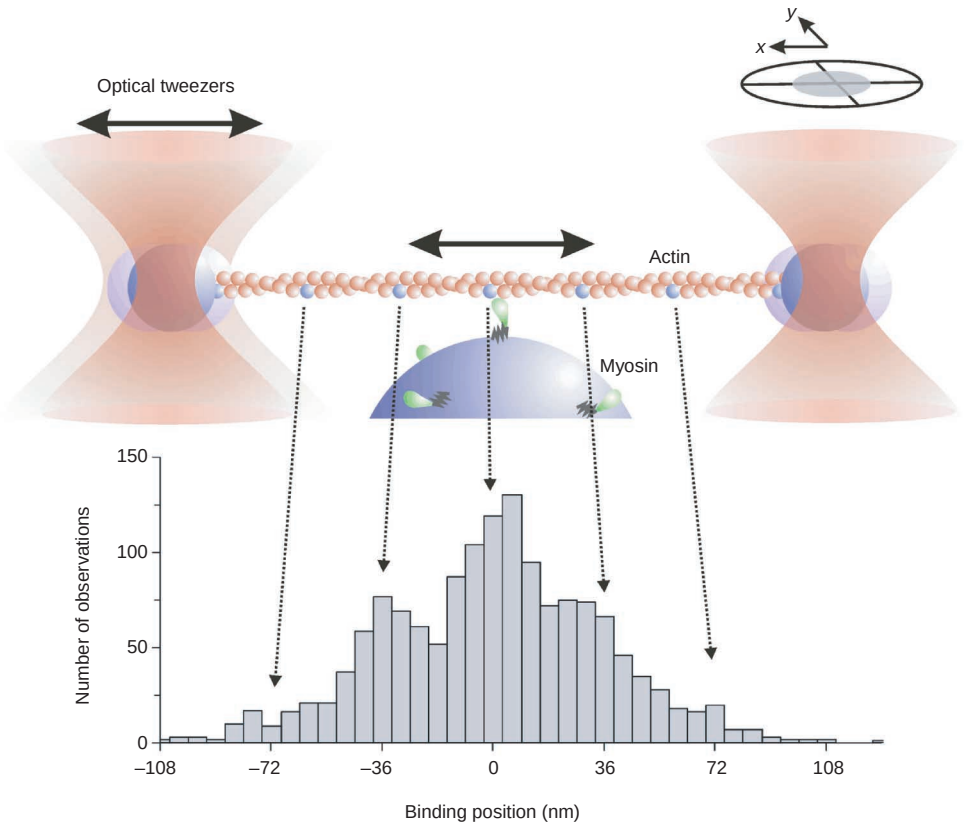

Figure 4 **Actin scanning experiment.** An actin filament was moved back and forth past a single MVS1 molecule to test whether binding occurred preferentially at specific sites along the filament. One optical tweezer was moved sinusoidally at 100 Hz with a peak-to-peak amplitude of 250 nm. The pairwise difference in amplitude between adjacent binding events was measured and plotted as a histogram. Binding events cluster at multiples of 36 nm, which is the same distance as the helical pseudorepeat of actin. For conditions see Methods; 5 μM ATP; $n = 1468$.

made with TPMV while processing along actin and would not be evident in experiments with MVS1. This would require that the helical twist of the actin filament impose a periodic energy profile with minima at binding positions with lowest azimuthal distortion to the myosin V molecule (that is, the actin helical pseudorepeat distance of 36 nm). The working stroke produced by the bound head would then serve to position the unbound head in an unstable region where diffusion is biased in the forward direction.

Data from the actin-scanning experiment are consistent with a simple model in which there is a sinusoidal energy landscape for binding probability along each of the two actin protofilaments (Fig. 5B). The derivative of the free-energy profile (shown in Fig. 5Be) would yield the diffusive force acting on an unbound TPMV head. This causes it to diffuse forward by a distance (x) of ~10–15 nm, to the next target actin monomer (producing an overall step size of 36 nm). A consequence of this model is that the TPMV molecule must become internally strained to enable both heads to bind. Knowing the mechanical properties of the system, we can calculate the average time that it would take for the unbound head to diffuse this distance. First, the internal strain energy, U, is found from a knowledge of the stiffness, κ_m, of MVS1 to be one half $\kappa_m x^2 \approx 12$ pN nm $\equiv 3k_bT$. Second, the relaxation time, τ, of the unbound TPMV head in water is given by $\tau = 6\pi\eta r/\kappa_m \approx 1$ μs. Third, the Kramer[18,19] first-passage time, t_k, is therefore given by $t_k = \tau\sqrt{(\pi/4)}\sqrt{(k_bT/U)}\exp(U/k_bT) \approx 0.1$ ms. This is only a small fraction of the dwell time at each processive step. We suspect that the intervals of reduced stiffness observed immediately before steps (Fig. 5A) betray this diffusive process. We know that whereas the unbound head undergoes such diffusive motion, the bound head must have product in its catalytic site; otherwise rapid binding of ATP to the acto-myosin V rigor complex would cause the head, and hence the entire molecule, to dissociate. When the free head binds, the internal molecular strain that it produces should affect chemical kinetics on the rear head by a factor of up to tenfold ($\exp(-U/k_bT)$). We compared the dwell times of single interactions of TPMV with the dwell times observed in 'staircases'. At saturating ATP (>0.1 mM ATP) and low load conditions (external forces <2 pN) the dwell times of single interactions were significantly longer (107 ± 11 ms) than the dwell times observed in 'staircases' (67–75 ms; Fig. 3e). This indicates that the rate-limiting step at saturating ATP is accelerated about twofold by internal strain. We suspect that the strain-dependent step is either ADP release or an ADP isomerization occurring on the rear head and at low load this produces the 5-nm working-stroke transition from phase 1 to phase 2 observed with both MVS1 and TPMV (see, for example, Fig. 2b).

A related model for a strain-dependent ADP release mechanism has been suggested for two-headed smooth-muscle myosin, with ADP release being accelerated from a cross-bridge bearing negative strain and slowed under positive strains[20].

We conclude that the processive movement of mouse myosin V along the 36-nm actin helical repeat is achieved as follows: head 1 binds to actin with ADP-P_i in its catalytic site, phosphate leaves and a 20-nm working stroke is produced. Head 2 then undergoes a diffusive search along the actin helix and binds preferentially to the actin monomer that presents least azimuthal distortion (36 nm downstream from head 1). Upon binding of head 2, internal

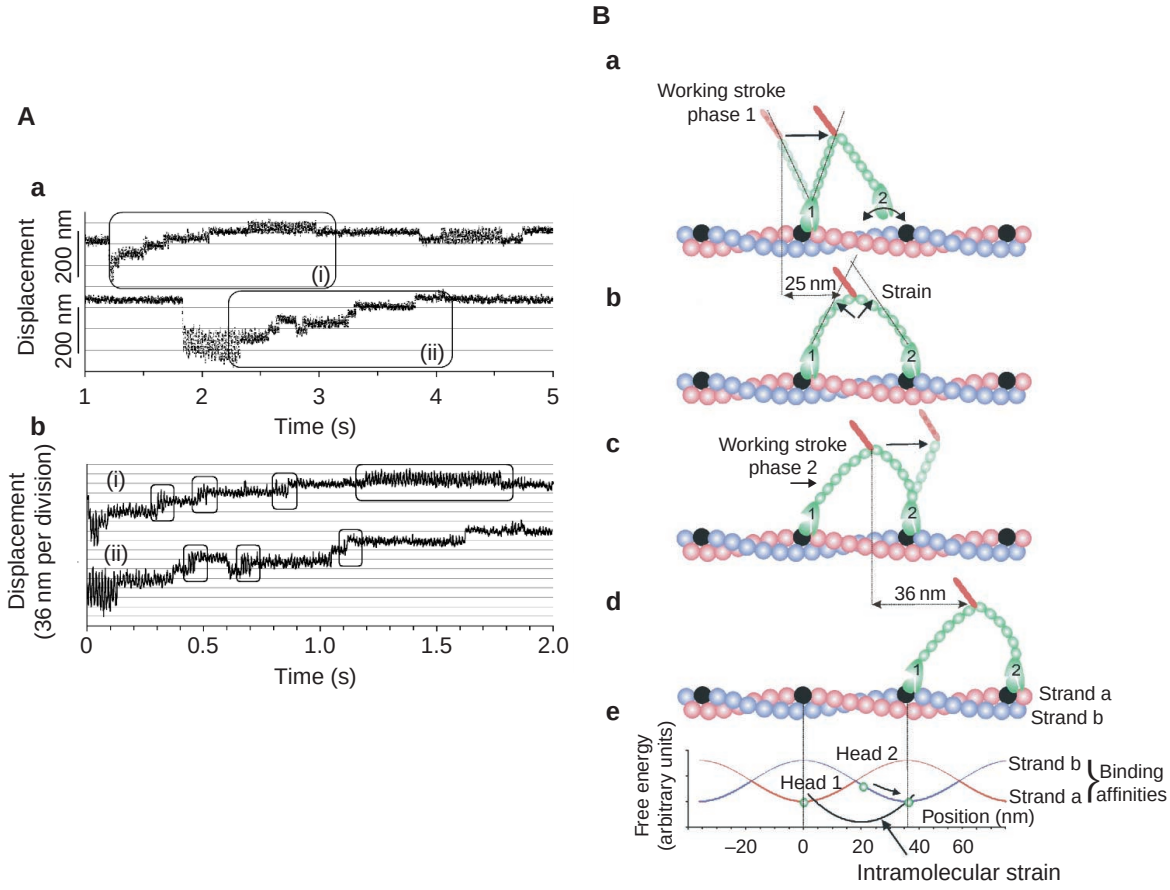

Figure 5 **Stiffness measurements with TPMV and a model for processive myosin movement. A**, Stiffness measurements with TPMV and 100 μM ATP. **a**, Stiffness was measured by driving one bead with a sinusoidal forcing function at 75 Hz and a peak-to-peak amplitude of 250 nm; the position of both beads over time was recorded. The time-dependent position of the driven bead is shown. Positional data from boxes (i) and (ii) are shown on an expanded time scale in **b**. Note the low-stiffness intervals (high-amplitude movements marked by boxes) of variable duration immediately preceding many of the transitions between levels. The low-stiffness intervals are of longer duration at higher forces. The mid-position during such low-stiffness intervals was ~20 nm above the previous level, which is similar to the amplitude of the first phase of the working stroke measured for MVS1. **B**, Model for processive myosin movement along the 36-nm helical repeat of actin. **a**, Head 1 attaches and produces a working stroke of 20 nm, probably coupled to the release of phosphate (straight arrow). While ADP is still bound to head 1, the unbound head 2 explores the energy landscape of the actin filament surface (shown in **e**), driven by Brownian motion (curved arrow). Note that the working stroke of head 1 has positioned head 2 in an unstable region such that it experiences a diffusional force (which would be the derivative of the sinusoidal free-energy landscape (**e**)) directed towards the next preferred binding position (dotted vertical line). **b**, Head 2 binds, causing internal strain (elastic strain energy, parabolic function of position; black parabola in e). **c**, The elastic strain gates the release of ADP from head 1 by accelerating the second phase of the working stroke (5 nm), which then relieves some of the internal strain. Subsequent binding of ATP to head 1 causes it to detach and head 2 to undergo its working stroke so that the next mechanical step can be made. **d**, At low ATP concentration, processively moving myosin V would dwell predominantly with ADP bound to the front head and the rear head in rigor state, as shown in **c**. At saturating ATP, myosin V would probably dwell with ADP bound to both the front and the rear head, as shown in **b**.

molecular strain accelerates the loss of product from head 1 and initiates three rapid events: (1) a second conformational change (of 5 nm) in head 1 followed by a loss of ADP, (2) the binding of ATP and the dissociation of head 1; (3) a loss of phosphate from head 2 and the production of the 20-nm working stroke, positioning head 1 now to make its diffusive search for the next actin target site. Crucial to the mechanism are the following: (1) the myosin V working stroke is not commensurate with the helical repeat, which means both that there must be a diffusive search for the next target actin binding site and that there is internal molecular stress when both heads are bound; and (2) the second phase of the working stroke acts as a gate that is opened by the internal strain produced by the binding of head 2. This makes the chemical cycles of the two heads cooperative and increases the processivity. We have modelled this mechanism with Monte Carlo methods (data not shown) and confirmed that processivity increases significantly if the biochemical cycles of the two heads interact in the way that we propose.

Myosin V is involved in membrane trafficking processes such as the trafficking of melanosomes[1], smooth endoplasmic reticulum[2] and neuronal vesicles in dendritic spines[4]. Actin filaments forming the cytoskeletal scaffolding in hippocampal dendritic spines are between 10 and 1,000 nm long[21]. With a processivity number of ~20, a single myosin V molecule would be able to transport vesicles along actin for ~720 nm, which is similar to the average filament length in dendritic spines. □

Methods

Protein preparations

Expressed mouse myosin V fragment S1 (MVS1) and tissue-purified myosin V from mouse brain (TPMV) were prepared as described[12,13]. Both preparations translocated actin filaments in sliding-filament assays at 0.2–0.4 μm s^{-1}. Rhodamine-phalloidin-labelled F-actin and *N*-ethylmaleimide (NEM)-modified rabbit myosin were prepared by standard methods[14].

Optical trapping conditions

We used a transducer based on optical tweezers that was built around a Zeiss Axiovert microscope[11,14]. Experiments were performed with flow cells made from a microscope slide and pieces of coverslip[11]. Glass microspheres (1.7 μm) were applied to the coverslip surface as a suspension in 0.1% v/w nitrocellulose/amyl acetate. The nitrocellulose surface was precoated with 10 μg ml^{-1} BSA (Sigma). Then MVS1 or TPMV was allowed to bind to the coverslip surface, with 10–50 ng ml^{-1} of protein in buffered salt solution. (containing, in mM, 25 KCl, 25 imidazole, 4 $MgCl_2$ and 1 EGTA; pH 7.4 at 23 °C). With some TPMV preparations a significantly higher number of processive interactions were observed when TPMV was applied to the experimental chamber in the presence of 10 μM calcium. The solution was replaced with one containing rhodamine-phalloidin-labelled actin filaments and 1.1 μm polystyrene beads that had been precoated with NEM-modified myosin. The buffered salt solution was supplemented with (in mM) 2 creatine phosphate, 20 dithiothreitol, 0.02–0.1 ATP and (in mg ml^{-1}) 1 creatine phosphokinase, 0.5 BSA, 3 glucose, 0.1 glucose oxidase and 0.02 catalase. In the experiments, a single actin filament was attached at either end to a 1.1-μm polystyrene bead held in optical tweezers and positioned near a stationary glass microsphere. Interactions between actin and the surface-bound myosin V were monitored by casting the image of the polystyrene beads onto two four-quadrant photodetectors. With the actin filament held taut, but in the absence of myosin binding, the root-mean-square (r.m.s.) amplitude of Brownian motion was $(k_b T/\kappa_{trap})^{0.5} \approx 12$ nm (where $k_b T$ is the thermal energy and κ_{trap} is the combined stiffness of the optical tweezers, $\kappa_{trap} = 0.015–0.02$ pN nm^{-1}). When myosin bound to actin, the motion of the beads parallel to the filament axis was restrained by an additional stiffness, κ_{add}, making the total system stiffness $\kappa_{tot} = \kappa_{trap} + \kappa_{add}$, which reduced the r.m.s. amplitude to $(k_b T/\kappa_{tot})^{0.5}$. Brownian motion showed a lorentzian power-density distribution with a roll-off frequency, f_c, of $\kappa_{tot}/2\pi\beta \approx 500$ Hz (where $\beta = 6\pi\eta r$; η is solution viscosity and r is combined bead radius, 1.1 μm).

To ensure that the records obtained were derived from a single myosin molecule, we adjusted the surface density by diluting the myosin-containing solution such that binding events were separated by long intervening periods of free bead diffusion and that ~70% of the stationary beads tested showed no interactions with the actin filament.

RECEIVED 27 JUNE 2001; 17 SEPTEMBER 2001; ACCEPTED 29 OCTOBER 2001;
PUBLISHED 10 DECEMBER 2001.

1. Reck-Peterson, S., Provance, D. W., Mooseker, M. S. & Mercer, J. A. Review: class V myosins. *Biochim. Biophys. Acta* **1496,** 36–51 (2000).
2. Cheney, R. E. *et al.* Brain myosin V is a two-headed unconventional myosin with motor activity. *Cell* **75,** 13–23 (1993).
3. Sellers, J. R. *Myosins* (Oxford Univ Press, 1999).
4. Miller, K. E. & Sheetz, M. P. Characterization of myosin V binding to brain vesicles. *J. Biol. Chem.* **275,** 2598–2606 (2000).
5. Mehta, A. D. *et al.* Myosin V is a processive actin-based motor. *Nature* **400,** 590–593 (1999).
6. Rief, M. *et al.* Myosin V stepping kinetics: a molecular model for processivity. *Proc. Natl Acad. Sci. USA* **97,** 9482–9486 (2000).
7. Sakamoto, T. I., Amitani, E., Yokota & Ando, T. Direct observation of processive movement by individual myosin V molecules. *Biochem. Biophys. Res. Commun.* **272,** 586–590 (2000).
8. Walker, M. *et al.* Two-headed binding of a processive myosin to F-actin. *Nature* **405,** 804–807 (2000).
9. De La Cruz, E. M., Wells, A. L., Rosenfeld, S. S., Ostap, E. M. & Sweeney, H. L. The kinetic mechanism of myosin V. *Proc. Natl Acad. Sci. USA* **96,** 13726–13731 (1999).
10. Schnitzer, M. J. & Block, S. M. Statistical kinetics of processive enzymes. *Cold Spring Harb. Symp. Quant. Biol.* **60,** 793–802 (1995).
11. Molloy, J. E. *et al.* Single molecule mechanics of heavy meromyosin and S1 interacting with rabbit or *Drosophila* actins using optical tweezers. *Biophys. J.* **68,** 298s–305s (1995).
12. Wang, F. *et al.* Effect of ADP and ionic strength on the kinetic and motile properties of recombinant mouse myosin V. *J. Biol. Chem.* **275,** 4329–4335 (2000).
13. Cheney, R. E. Purification and assay of myosin V. *Methods Enzymol.* **298,** 3–18 (1998).
14. Veigel, C., Bartoo, M. L., White, D. C. S., Sparrow, J. C. & Molloy, J. E. The stiffness of rabbit skeletal, acto-myosin crossbridges determined with an optical tweezers transducer. *Biophys. J.* **75,** 1424–1438 (1998).
15. Molloy, J. E., Burns, J. E., Kendrick-Jones, J., Tregear, R. T. & White, D. C. S. Movement and force produced by a single myosin head. *Nature* **378,** 209–212 (1995).
16. Veigel, C. *et al.* The motor protein myosin-I produces its working stroke in two steps. *Nature* **398,** 530–533 (1999).
17. Wray, J. Filament geometry and the activation of insect flight muscles. *Nature* **280,** 325–326 (1979).
18. Kramers, H. A. Brownian motion in a field of force and the diffusion model of chemical reactions. *Physica* **7,** 284–304 (1940).
19. Howard, J. *Mechanics of Motor Proteins and the Cytoskeleton* (Sinauer Associates, Sunderland, Massachusetts, 2001).
20. Berger, C. E.M, Fagnant, P. M., Heizmann, S., Trybus, K. M. & Geeves, M. A. ADP binding induces and asymmetry between the heads of unphosphorylated myosin. *J. Biol. Chem.* **276,** 23240–23245 (2001).
21. Rao, A. & Craig, A. M. (2000). Signaling between the actin cytoskeleton and the postsynaptic density of dendritic spines. *Hippocampus* **10,** 527–541 (2000).
22. Huxley, A. F. (1957). Muscle structure and theories of contraction. *Progr. Biophys. Biophys. Chem.* **7,** 255–318 (1957).

ACKNOWLEDGEMENTS

We thank E. Harvey for technical assistance, J. A. Hammer III for kindly supplying the MV clone, J. C. Sparrow, D. C. S. White, R. S. Adelstein, J. Trinick, P. J. Knight and E. Homsher for critical reading of the manuscript, and BBSRC, the Royal Society, the Wellcome Trust and the NIH for grant support.
Correspondence and requests for materials should be addressed to C.V and J.R.S.